Acta Metall. Sin. (Engl. Lett.), 2015, **28**(3), 289–294
DOI 10.1007/s40195-014-0195-3

The Change of Orientation Relationships Between Austenite and α′-Martensite During Deformation in High Manganese TRIP Steel

Hai-Yan Yang · Jing Li · Ping Yang

Received: 24 June 2014 / Revised: 21 July 2014 / Published online: 8 January 2015

Abstract In situ observation of electron backscattering diffraction technique was used to evaluate the orientation relationships between austenite and α′-martensite (α′-M) for high manganese transformation-induced plasticity steel. It was noted that different from the thermal martensite, which well obeyed K–S relationship with austenite, the orientation relationship between deformation-induced α′-M with austenite changed during deformation, namely K–S and N–W relations coexisted. No clear differences existed between α′-M variants with two kinds of relationships in terms of martensitic orientation, shape and the misorientation between α′-M variants. And this phenomenon happened in almost all austenitic grains with different orientations investigated in this study. An atom displacement mechanism through conjugate complex slips of partial dislocations in the distorted fcc lattice was applied in this article to interpret the coexistence of K–S and N–W relationships.

KEY WORDS: In situ observation; Orientation relationship; Electron backscattered diffraction technique (EBSD); Martensitic transformation; High manganese TRIP steel

1 Introduction

Transformation-induced plasticity (TRIP) effect offers high manganese steels with high ductility while maintaining high strength. Thus, high manganese TRIP steels are considered as good material candidates for future automotive industry applications [1, 2]. Martensitic transformation will lead to a reproducible orientation relationship (hereafter abbreviated to OR or ORs) between the parent and product phase [3]. And preferred OR is an important part of the study on phase transformation crystallography [4]. It is the theoretical foundation to understand phase transformation mechanisms [5] and to control the microstructure of multiphase materials [6]. Phase boundaries play an important role in multiphase steels. Zhang et al. [7] examined the structure of the bcc/fcc iron phase boundaries in Nishiyama–Wassermann (N–W) and Kurdjumov–Sachs (K–S) relationships using molecular dynamics simulation and found that the phase boundary with N–W relation had the lower energy than that with K–S relation and dual-phase model in N–W relation was twice higher in stiffness than that in K–S relation. TRIP effect relates to the interaction between phase transformation and deformation which may change the ORs between the parent and the product phases. Three common correspondence relationships, namely the K–S, N–W and Greninger–Troiano (G–T), are cited in recent researches about relationships between austenite and its product phases in Fe–Ni alloys [8], duplex steel [9] and TRIP steel [10, 11]. And studies about the ORs between the austenite and the strain-induced martensite have been reported in different alloys [12–14], but few in high manganese TRIP steels. Thus, the purpose of the present study is to investigate the difference between

Available online at http://link.springer.com/journal/40195

H.-Y. Yang · J. Li · P. Yang (✉)
School of Materials Science and Engineering, University of Science and Technology Beijing, Beijing 100083, China
e-mail: yangp@mater.ustb.edu.cn

thermal and deformation-induced α′-M in terms of the ORs with austenite and then determinate the ORs between austenite and deformation-induced α′-M in high manganese TRIP steel by the combination of in situ observation and orientation mapping based on EBSD technique.

2 Materials and Methods

High manganese TRIP steel with Fe–17.22Mn–2.87Si–0.48Al–0.022C (in wt%) was used in this study, and a tensile sample with a gauge length of 9 mm and a cross-section dimension of 3 mm × 1 mm was cut from the hot-forged steel and then heated at 1,323 K for 10 min followed by water quenching. Three phases existed at room temperature before deformation, namely metastable austenite, ε-martensite (ε-M) and α′-M. And the volume fractions of the austenite, ε-M and α′-M, which were achieved from the statistics of 24 EBSD areas before deformation, were 49.8%, 48.3% and 1.9%, respectively (Fig. 1). The sample was mechanically polished and then etched in 4% nital solution.

Seven areas were marked on surface of the etched specimen for in situ investigation using a micro-Vickers hardness tester before applying tensile load as shown in Fig. 1. The specimen was uniaxially stretched at room temperature at a rate of 0.1 mm/min using an in situ deformation stage installed in a CS5000 scanning electron microscope (SEM). Zeiss Ultra 55 field-emission gun scanning electron microscope (FE-SEM) equipped with HKL EBSD systems was applied before and after deformation to evaluate the ORs.

3 Results

The OR between the austenite and martensite can be represented as axis/angle pair $<d>\omega$. The most referenced ORs are the K–S <0.18 0.18 0.97> 42.85°, the N–W <0.2 0.08 0.98> 45.98° and the G–T <0.97 0.19 0.13> 44.23° [10]. The axes can be simplified as <116>, <105> and <3 2 16>, respectively. It has been demonstrated that the G–T relation approximately locates in the middle of the connection line between K–S and N–W ORs in Euler orientation subspace [15] and a G–T variant is present approximately midway between each pair of adjacent K–S and N–W variants [4]. Moreover, some deviation from ideal ORs will be induced by deformation. Thus, the G–T relation is regarded as an intermediate, but not independent, OR in our article. In the present work, the OR investigation was conducted by calculating the misorientations between the austenite and the nearest neighboring α′-M and comparing them to the common ORs mentioned above. To calculate the misorientations, the measured orientations of the austenite and the nearest neighboring α′-M were represented in the format of Euler angles. And, in consideration of the angular accuracy of EBSD system (about 1°) and the calculation error, a 2.5° tolerance is employed for all the ORs in the following sections. Thus, the value ranges of three relationships are listed in Table 1.

3.1 Change of OR Between Thermal α′-M and the Austenite During Deformation

251 and 210 misorientation axis/angle pairs, respectively, are calculated to evaluate the change of orientation

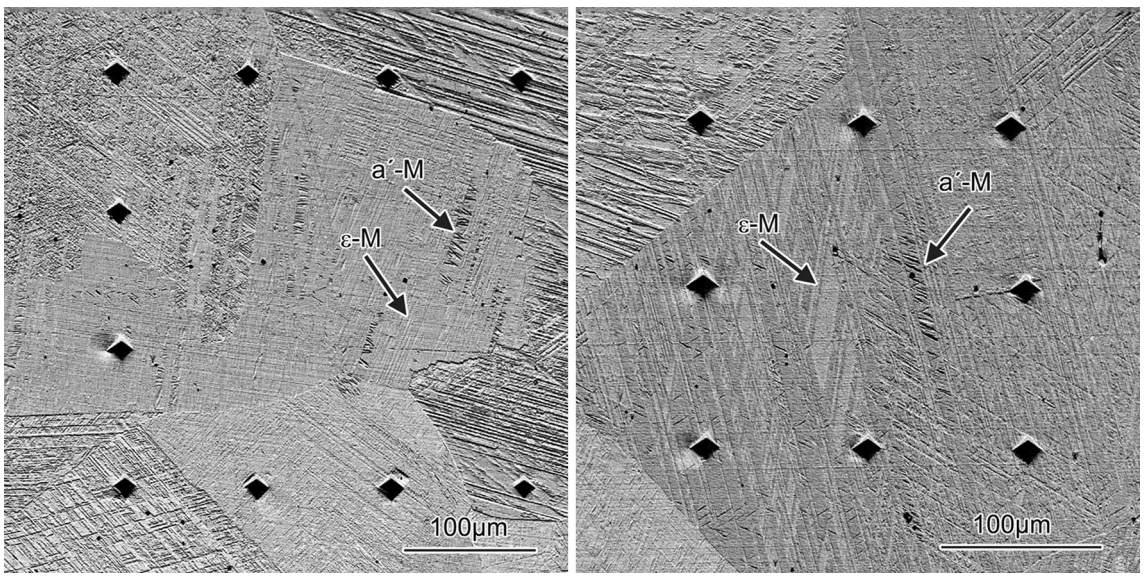

Fig. 1 SEM micrographs of marked areas on the surface of specimen before deformation

Table 1 The value ranges of three kinds of ORs investigated in this work

Orientation relationship	Deviation
K–S	<1 1 6> 40.35°–45.35°
N–W	<1 0 5> 43.48°–48.48°
G–T	<3 2 16> 41.73°–46.73°

relationship between austenite and thermal α′-M of the sample subjected to a tensile strain of 10% as displayed in Fig. 2. The misorientation angle and rotation axis focus on 42.85° and <116> very well indicating that the K–S relationship is obeyed perfectly before deformation, despite slight scatter exists in Fig. 2a. The internal stress during cooling and measurement error may be responsible for this slight scatter (about 1.5°). Due to the rotation of orientation during tension, the distribution of the misorientation angles and the rotation axes, which still focus on 42.85° and <116>, just become more scattered. Although N–W relation is presented in Fig. 2c, f, the proportions of it are only 0.4 and 5%, respectively, which can be attributed to the calculation error and be ignored reasonably. Therefore, the K–S relationship is dominant between austenite and thermal α′-M during the deformation of 10% as shown in Fig. 2c, f which is classified according to Table 1.

3.2 ORs Between Austenite and Deformation-Induced α′-M

Figure 3 presents the 358 axis/angle pairs of misorientations between the austenite and deformation-induced α′-M. The statistical method is the same as in Fig. 2. The peak of

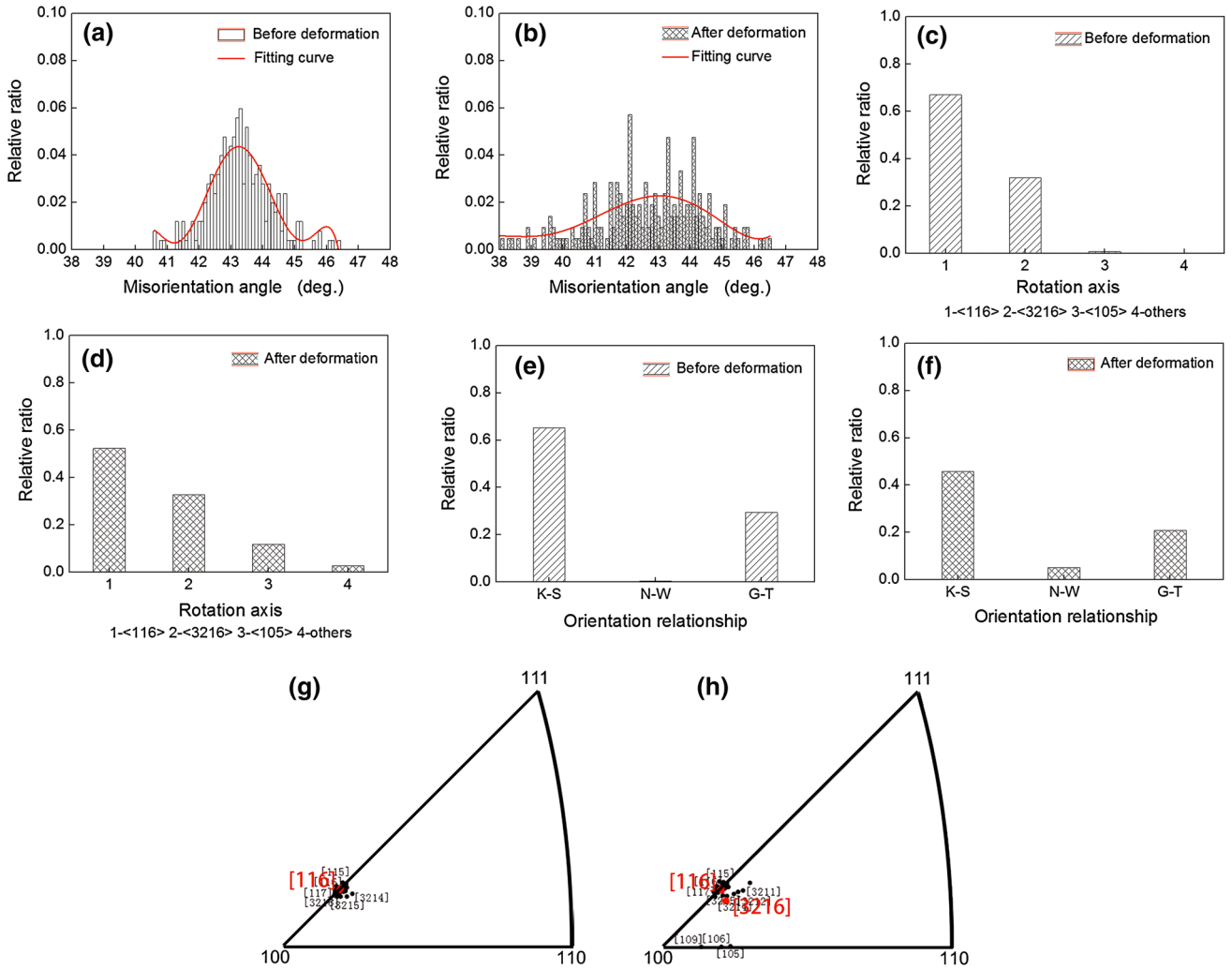

Fig. 2 Statistic results of the orientation relationships between the austenite and thermal α′-M: **a**, **b** distribution of misorientation angle before and after deformation; **c**, **d** rotation axis of the three ORs mentioned above before and after deformation; **e**, **f** ORs before and after deformation; **g**, **h** distribution of rotation axis showed in stereographic projection triangle before and after deformation

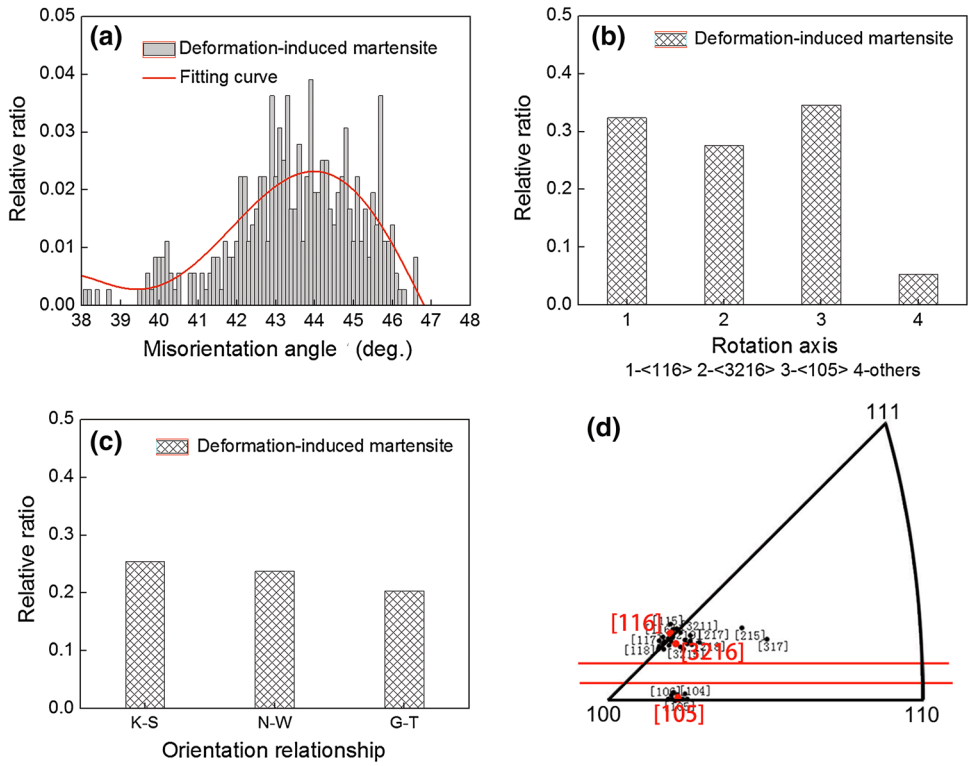

Fig. 3 Statistic results of the orientation relationships between the austenite and deformation-induced α′-M: **a** distribution of misorientation angle; **b** rotation axis of the three terms mentioned above; **c** orientation relationship; **d** distribution of rotation axis showed in stereographic projection triangle

misorientation angles locates at 44.5° which deviates distinctly from the 42.85° for K–S relationship, as displayed in Fig. 3a. The rotation axes focus on <116> and <105>, and no transition exists between them as the red lines shown in Fig. 3d, indicating the appearance of new orientation relationship. Figure 3c, based on the value ranges of three ORs listed in Table 1, shows that both the K–S (25.4%) and N–W (23.7%) relationships are obeyed and G–T is an intermediate OR when the austenite transforms into α′-M during deformation.

3.3 Characteristics of α′-M Variants with Two Kinds of Relationships

Figure 4 displays the EBSD mappings of α′-M variants with K–S and N–W relationships in one of the seven marked areas. And Fig. 4b is the magnification of the region inside square in Fig. 4a after deformation. It is noted that similar α′-M variants (marked by number 1 and 2 in Fig. 4c) form at two sides of the austenitic twin grain (black line in Fig. 4b). The ORs between them and the austenite, however, are different which are judged by the method mentioned above, and 1 exhibits K–S and 2 N–W relations. As far as the misorientations between α′-M variants are concerned, the α′-M variants with N–W relationship always exist separately and no Σ3 and Σ11 misorientations exist between them, which generally present among α′-M variants with K–S relationship. However, the Σ3 and Σ11 misorientations may not be accurately indicated due to the orientation rotation caused by deformation. So the misorientations between α′-M variants may not be regarded as a reliable foundation to distinguish α′-M variants with N–W relation from those with K–S relation. And the shapes of α′-M variants are not significantly different as shown in Fig. 4c.

The austenitic orientation, indexed as the tension axis (TA) direction, is showed in a [100]-[110]-[111] standard stereographic triangle, as displayed in Fig. 4d. The black square spots denote the orientations of austenitic grains which contain α′-M variants with both K–S and N–W relationships, while the red square spots represent the orientations of austenitic grains which only contain α′-M variants with K–S relationship. It is noted that the K–S and N–W relations coexist in most austenitic grains whose orientations distribute randomly. And further analysis about the orientations of α′-M variants with K–S and N–W relationships is displayed in Fig. 4e, f. It is observed that the orientations of α′-M variants with N–W relationship close to $<100>_{\alpha'}$ and $<110>_{\alpha'}$//TA which are only slightly different from those of α′-M variants with K–S relationship. Thus,

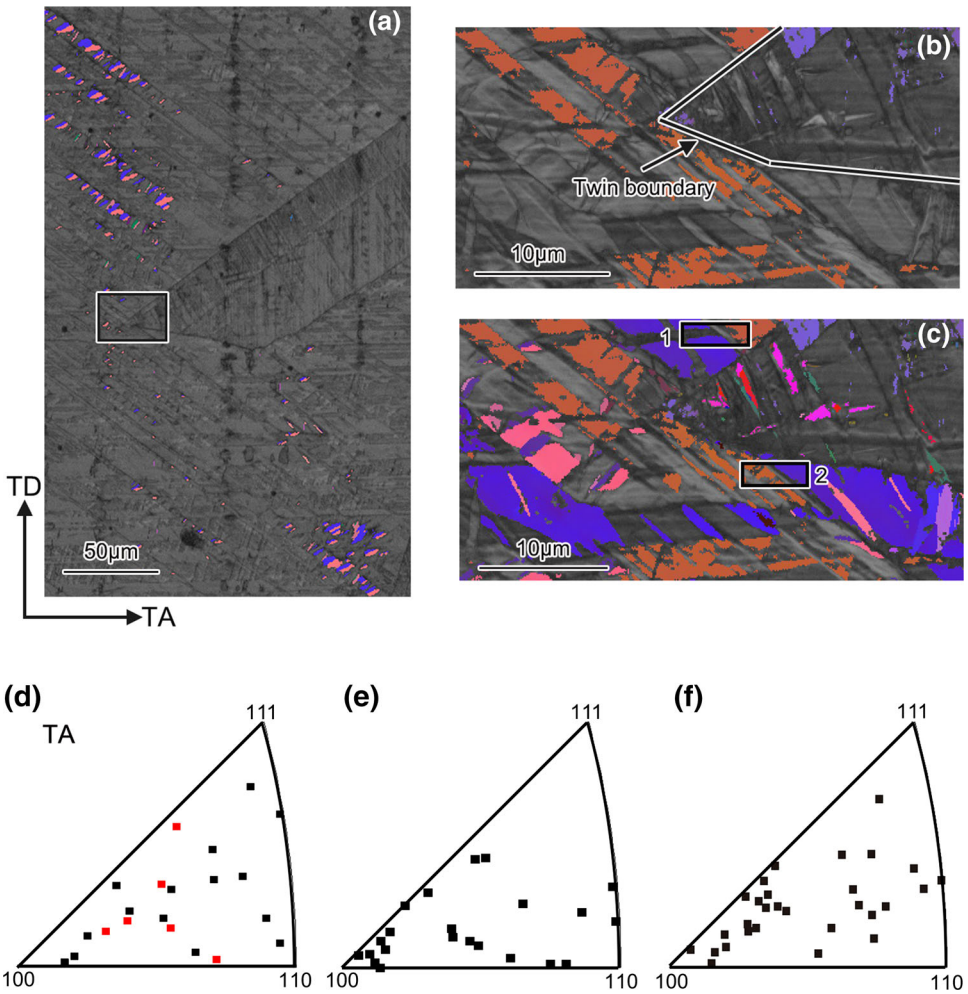

Fig. 4 EBSD orientation maps and the orientations of the austenitic grains and α′-M variants: **a** orientation map of α′-M before deformation (*colors* α′-M variants, *gray* austenite and ε-M); **b** magnifying orientation map of the region inside *square* in **a** (*colors* austenite with twin relationship, *gray* α′-M and ε-M); **c** orientation map of α′-M and austenite (*orange and light purple* austenite (the same as **b**), other (*colors* α′-M, *gray* ε-M); **d** the inverse pole figure for the TA direction of austenitic grains investigated in this study; **e**, **f** the inverse pole figure of α′-M variants with N–W relationship and K–S relationship, respectively

there is no distinct difference between the α′-M variants with K–S and N–W relationships as regards the orientation, misorientation between α′-M variants and shape in this study.

4 Discussion

As mentioned above, the α′-M variants with N–W relation are not clearly different from those with K–S relation in terms of orientation, shape and misorientations. Thus, we attempt to explain the coexistence of K–S and N–W relationships by using the dislocation slip mechanism proposed by Lin [16]. The key point of this mechanism is that the fcc → bcc lattice variation is the consequence of relative position changes between atoms which is caused by the shears in combination with different slip systems along $<112>_f/\{111\}_f$ in the distorted fcc lattice during martensite transformation. And the fcc lattice distortion may change the slip length of partial dislocation from 1/6<112> to $1/n<112>$. Two types of displacements happen in this process: One is the main shear displacement only along one slip system of $(1/m)$ $<112>_f/\{111\}_f$, and the other is the complex displacement $M = (1/n)$ $[<112>_{f1}/\{111\}_{f1} + <112>_{f2}/\{111\}_{f2}]$ $(n > 6)$, which is obtained by partial dislocations operated in two conjugate slip planes $\{111\}_f$. Then the K–S and N–W ORs can coexist by different combinations of main shear displacement and conjugate complex displacement.

The selected materials in Ref. [16] were composed of various alloy elements and a certain proportion of C atoms which would lead to distinctly distorted fcc lattice and then the coexistence of α′-M variants with K–S and N–W relationships during quenching. In the present work, the atomic radius of Fe and Mn is similar and only 0.022 wt% C atoms in high manganese TRIP steel, which would lead

to slight lattice distortion, so K–S relation is the only OR between thermal α'-M and austenite. However, tensile deformation would result in the distortion of austenitic lattices during martensitic transformation, followed by the combination displacements of partial dislocations mentioned above, and α'-M variants with K–S and N–W relationships can form simultaneously. And there is no doubt that further investigation is also needed to verify the accuracy of this explanation for our materials.

5 Conclusions

There exists distinct difference between thermal and deformation-induced α'-M in terms of orientation relationships. K–S relationship is the main relationship for thermal α'-M under a tensile straining of 10%. However, deformation-induced α'-M variants with K–S and N–W relations coexist during deformation. And no clear difference exists between α'-M variants with N–W relationship and those with K–S relationship according to EBSD orientation data. The partial dislocations make an atom displacement through the combination of the main shear displacement only along one $\{111\}_f$ with complex slips on two conjugate slip planes $\{111\}_f$ in the distorted fcc lattice.

Acknowledgments This work was financially supported by the National Natural Science Foundation of China (No. 51271028).

References

[1] C.Y. Choi, I. Kim, Y. Kim, Y. Park, Korean J. Metal Mater. **50**, 136 (2012)
[2] O. Bouaziz, H. Zurob, M. Huang, Steel Res. Int. **84**, 937 (2013)
[3] N. Takayama, G. Miyamoto, T. Furuhara, Acta Mater. **60**, 2387 (2012)
[4] Y. He, S. Godet, P.J. Jacques, J.J. Jonas, Acta Mater. **54**, 1323 (2006)
[5] S. Zaefferer, J. Ohlert, W. Bleck, Acta Mater. **52**, 2765 (2004)
[6] S. Morito, H. Tanaka, R. Konishi, T. Furuhara, T. Maki, Acta Mater. **51**, 1789 (2003)
[7] Y. Zhang, Y. Zhao, F.C. Zhang, Adv. Mater. Res. **479**, 601 (2012)
[8] H. Kitahara, R. Ueji, M. Ueda, N. Tsuji, Y. Minamino, Mater. Charact. **54**, 378 (2005)
[9] C. Wang, W. Cao, J. Shi, C. Huang, H. Dong, Mater. Sci. Eng. A **562**, 89 (2013)
[10] K. Verbeken, L. Barbe, D. Raabe, ISIJ Int. **49**, 1601 (2009)
[11] B. Verlinden, P. Bocher, E. Girault, E. Aernoudt, Scr. Mater. **45**, 909 (2001)
[12] S. Martin, S. Richter, A. Poklad, H. Berek, S. Decker, U. Martin, L. Krüger, D. Rafaja, J. Alloys Compd. **577**, S578 (2013)
[13] X.M. Zhang, E. Gautier, A. Simon, Acta Metall. **37**, 487 (1989)
[14] H. Guo, X. Gao, Y. Bai, M. Enomoto, S. Yang, X. He, Mater. Charact. **67**, 34 (2012)
[15] G. Nolze, Cryst. Res. Technol. **41**, 72 (2006)
[16] B.J. Lin, Acta Metall. Sin. **18**, 350 (1982). (in Chinese)